Russian Chemical Reviews **76** (6) 493 – 506 (2007) © 2007 Russian Academy of Sciences and Turpion Ltd

DOI 10.1070/RC2007v076n06ABEH003715

Quantum beats in radical pairs

V A Bagryansky, V I Borovkov, Yu N Molin

Contents

I.	Introduction	493
II.	The nature and detection of quantum beats in radical pairs	493
III.	Theory of quantum beats in recombination luminescence of spin-correlated radical ion pairs	496
IV.	Spectroscopy of quantum beats in radical pairs	499
V.	Conclusion	505

Abstract. Possible fields of application of the phenomenon of quantum beats in spin-correlated radical pairs in studies of the properties of short-lived radicals (lifetimes of up to a few nanoseconds) in liquid solutions are considered. The theoretical approaches to the description of this phenomenon and modern experimental data are analysed. The bibliography includes 82 references.

I. Introduction

Shortly after the discovery of chemically induced dynamic nuclear polarisation (CIDNP) in the late 1960s it was established that the course of radical reactions in solutions may be affected by external magnetic fields, resonance microwave radiation and hyperfine interactions (magnetic isotope effect). The new field of research on the effects of electron and nuclear spin dynamics on elementary chemical reactions is for brevity called 'spin chemistry' or 'dynamic spin chemistry'. Recent advantages, research potential and specific features of this field of chemical science have been well documented (see monographs [1–4] and reviews [5–21]).

Most phenomena studied by spin chemistry are due to dynamic (not associated with paramagnetic relaxation) transitions between different states of electron spins in a radical pair (RP) emerged in a coherent (singlet or triplet) spin state. Corresponding methods of investigation also employ this feature. These dynamic transitions, or quantum beats, are similar to quantum beats in other systems, which allows spin chemistry to be considered as a 'companion' to yet another new avenue of research, namely, femtochemistry, and to some spectroscopic methods of investigations that also utilise quantum interference. In both spin chemistry and femtochemistry the quantum beats in the populations of reactant states modulate the yield of reaction products. To describe these phenomena, one should allow for the oscillation phase of the wave function. This unusual, for chemistry, feature offers basically new opportunities for control of chemical reactions through variation of the phase relations in the wave packet by varying external factors. In addition, frequency analysis of quantum beats provides information on the properties of reacting species and offers new horizons for experimentalists.

Most experimental approaches used in spin chemistry involve analysis of time-average manifestations of the spin evolution in RPs. A typical example is provided by measurements of the magnetic field effect (dependence of the yield of final products of radical reactions on the magnetic field strength). The magnetic field affects positions of electron-spin energy levels and, as a consequence, the evolution of the spin state of the RP. Since the reaction is spin selective, the yield of reaction products changes with the magnetic field strength. The change in the product yield is thus an integrated 'fingerprint' of the temporal evolution of the spin state in the RP.

Development of pulsed methods of generation of radical pairs and relevant detection instruments with nanosecond temporal resolution permitted real-time monitoring of manifestations of quantum oscillations of the spin state in RP. In this review we will consider methods of detection of quantum beats based on recombination luminescence of RPs and the results of recent studies obtained by these techniques.

II. The nature and detection of quantum beats in radical pairs

1. A qualitative model

Dynamic singlet – triplet transitions in spin-correlated RPs are related to the quantum nature of electron spins. Spin-correlated pairs are produced upon rupture of chemical bonds or after ionisation of molecules. The total spin of the unpaired electrons remains unchanged, which means that the state (singlet or triplet) of a radical pair is the same as that of its precursor.

Quantum beats are due to the fact that the singlet and triplet states of RP are superpositions of several stationary states. In turn, this is due to the spin – orbit and hyperfine couplings in radicals. Quantum beats occur in any system whose states are coherent superpositions of stationary states.[22, 23] In the simplest case the initial state of a quantum system

$$|\Psi(0)\rangle = c_a|a\rangle + c_b|b\rangle,$$

V A Bagryansky, V I Borovkov, Yu N Molin Institute of Chemical Kinetics and Combustion, Siberian Branch of the Russian Academy of Sciences, ul. Institutskaya 3, 630090 Novosibirsk, Russian Federation. Fax (7-383) 330 73 50, tel. (7-383) 333 23 81, e-mail: vbag@kinetics.nsc.ru (V A Bagryansky), tel. (7-383) 330 97 92, e-mail: borovkov@kinetics.nsc.ru (V I Borovkov), tel. (7-383) 333 16 07, e-mail: molin@kinetics.nsc.ru (Yu N Molin)

Received 9 April 2007
Uspekhi Khimii **76** (6) 535 – 549 (2007); translated by A M Raevskiy

is a superposition of two vectors of the stationary states $|a\rangle$ and $|b\rangle$ of the system with the energies E_a and E_b, respectively (c_a and c_b are constants). At arbitrary instant $t > 0$, the state of the system is described by the vector

$$|\Psi(t)\rangle = c_a|a\rangle e^{-iat} + c_b|b\rangle e^{-ibt}, \quad (1)$$

where $a = E_a/\hbar$, $b = E_b/\hbar$. Let x be the operator of an observable quantity and let x have no explicit dependence on time. The average value of x in the state (1) is given by

$$\langle x(t)\rangle = \langle \Psi(t)|x|\Psi(t)\rangle = \quad (2)$$

$$= |c_a|^2 x_{aa} + |c_b|^2 x_{bb} + 2|c_a^* c_b x_{ab}| \cos[(a-b)t + \varphi].$$

The first two terms in the right side of Eqn (2) are the weight-average of x and the last term is the cross-term modulated by the frequency of the transition between the states a and b (here φ is the relative phase of the complex coefficients c_a and c_b). If the initial state is composed of more than two vectors of stationary states, the average value of the physical quantity is modulated by several frequencies.

The simplest example of quantum beats in a radical pair is provided by two noninteracting radicals differing in their isotropic g-factors. The energies of the stationary states of the pair in a strong magnetic field are shown in Fig. 1. Two states of the pair, with the energies E_1 and E_4, are the triplet states T_+ and T_-, whereas the other two states with the energies E_2 and E_3 are mixed states composed of the spin states S and T_0 taken with equal weights. This means that emergence of a radical pair in, *e.g.*, the singlet state will cause coherent population of two energy levels, E_2 and E_3. This will be accompanied by the onset of singlet–triplet oscillations at the frequency

$$\omega = \frac{\beta B}{\hbar}(g_1 - g_2),$$

corresponding to the difference E_2 and E_3. If isotropic hyperfine couplings (HFC) occur in the radicals, the oscillation frequencies are given by

$$\omega = \frac{\beta B}{\hbar}(g_1 - g_2) + \sum_{i1} a_{i1} m_{i1} - \sum_{i2} a_{i2} m_{i2},$$

where β is the Bohr magneton, B is the induction of external magnetic field, g is the g-factor, a_i is the constant of HFC with the ith nucleus, and m_i is the projection of the spin of the ith nucleus on the direction of the magnetic field; the subscripts '1' and '2' enumerate different radicals in the pair.

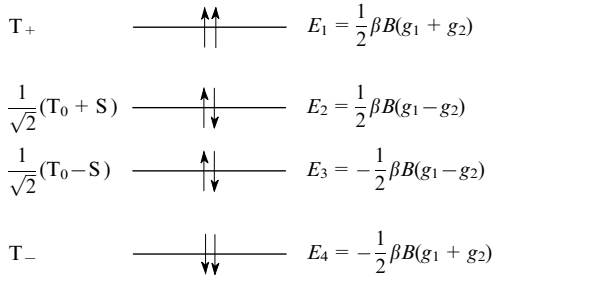


Figure 1. Energy levels of a radical pair comprising radicals with different g-factors in strong magnetic field.

The visual pattern of beats in an RP in a constant magnetic field (magnetic field strength much exceeds the constants of HFC in the radicals in the pair) is illustrated by the vector diagram shown in Fig. 2. The pair emerged in the singlet (S) spin state corresponds to the antiparallel orientation of the radical spins in the vector diagram (Fig. 2 *a*). Then, in a strong magnetic field the spins undergo precession about the magnetic field direction. However, the spin precession frequencies differ due to differences between the 'internal magnetic fields' owing to different spin–orbit and hyperfine interactions in radicals. As a result, the pair periodically goes to the T_0 state in which the vector sum of the spins differs from zero and is oriented normal to the magnetic field direction (Fig. 2 *b*).

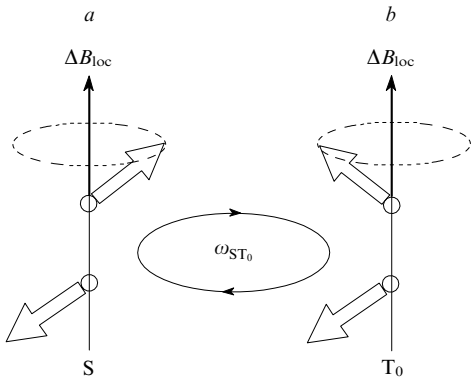


Figure 2. Vector diagram illustrating the onset of $S-T_0$ oscillations of the spin state of a radical pair in strong magnetic field.
Oscillations are due to the Larmor frequency difference between electron spins in different local magnetic fields.

2. Quantum beats in recombination luminescence

The possibility of experimental observation of quantum oscillations in RP is due to the fact that the yield of the products of recombination of the radicals in the pair depends on the total spin of the radicals at the instant of recombination. This means that oscillations of the singlet state population of the RP can be monitored by observing the kinetics of formation of the product of singlet recombination.

Experiments involving detection of recombination luminescence of radical ion pairs formed upon the action of a pulse of ionising radiation on non-polar solutions of electron donors and acceptors appeared to be the most fruitful for observation of quantum beats in the spin state of RP. The formation and recombination of radical ion pairs can be described by the following scheme:

$$\mathrm{Solv} \xrightarrow{\text{ionising radiation}} \mathrm{Solv}^{+\bullet} + \mathrm{e}^-, \quad (3)$$

$$\mathrm{Solv}^{+\bullet} + \mathrm{D} \longrightarrow \mathrm{Solv} + \mathrm{D}^{+\bullet}, \quad (4)$$

$$\mathrm{e}^- + \mathrm{A} \longrightarrow \mathrm{A}^{-\bullet}, \quad (5)$$

$$\mathrm{D}^{+\bullet} + \mathrm{A}^{-\bullet} \longrightarrow \mathrm{D} + \mathrm{A}^* \longrightarrow h\nu. \quad (6)$$

In the first stage (3), irradiation of dilute solutions of electron donors (D) and acceptors (A) causes ionisation of solvent molecules (Solv) and formation of a primary RP comprised of an electron and the solvent hole ($\mathrm{Solv}^{+\bullet}/\mathrm{e}^-$). Since the solvent molecule was in the singlet spin state before irradiation, the primary RP emerged upon ionisation is also in the singlet state.

This correlation also holds for the secondary pairs ($\mathrm{D}^{+\bullet}/\mathrm{A}^{-\bullet}$) if the rates of reactions (4) and (5) are higher than the rate of the singlet–triplet transition. To monitor the spin state of this pair using recombination luminescence, the electron donor or acceptor should be a luminophore with a rather short fluorescence time. Then, recombination (6) of the singlet radical pair resulting in a singlet-excited product A* (or D*) will be followed by emission of a fluorescence quan-

tum. As a consequence, the dynamic singlet – triplet transitions responsible for the oscillations of the singlet state population will induce modulation of the kinetics of recombination fluorescence. The recombination products of triplet pairs usually show no intense phosphorescence in solution.

Solutions in non-polar solvents are the most convenient systems for carrying out these experiments. The reasons are as follows. First, the separation between radical ions in the primary RPs generated in a non-polar medium is shorter than the Onsager radius. Therefore, they mainly recombine in a geminate fashion, *i.e.*, with the spin-correlated partners. Second, the solvation energy of the recombining radical ions in the non-polar medium is minimum, which favours the release of energy sufficient for recombination luminescence.[24] In addition, recombination immediately follows the first collision between radical ions irrespective of their spin state due to strong Coulomb attraction. Therefore, the effects of secondary collisions almost do not manifest themselves,[1] and the rate of formation of the singlet-excited products of recombination (6) can be represented by the product of the recombination rate to the singlet state population of the RP. This essentially simplifies the analysis of the kinetics of recombination luminescence in order to detect the quantum beats due to the singlet – triplet transitions in the spin state of the RP. Finally, the partners emerge and spend most time at a long distance from each other. Under these conditions the effect of the dipole – dipole and exchange interactions between partners can be ignored, which also essentially simplifies the theoretical description of the spin evolution in radical pairs.

3. Methods and instruments

Advances in detection of quantum beats were to a great extent due to the use of the single photon counting technique[25] for detection of recombination fluorescence. The method permits detection of fluorescence with high temporal resolution in high dynamic range of intensities ($>10^5$). Quantum beats are detected using radioactive sources of fast electrons[13, 14, 17, 26–48] and controllable sources of ionising radiation,[13, 14, 17, 41, 49–66] the latter providing a much higher performance of experimental installations.

At rather short excited-state lifetimes of recombination products, the experimental procedures involving detection of recombination fluorescence in fact detect the derivative of the accumulation kinetics of the product of the spin-dependent reaction. This improves the detection of quantum beats. An analogy is provided by radiospectroscopy. Namely, going to phase-sensitive detection (here, the derivative of the signal is recorded) provides enhanced resolution and improves the signal-to-noise ratio. Clearly, relevant mathematical processing of the data obtained by other methods will also allow quantum beats in reactions of spin-correlated RPs to be observed. Analysis of the temporal dependence of the fluorescence intensity ratio in nonzero and in zero magnetic field rather than the kinetics of recombination fluorescence offers additional advantages in the interpretation of experimental results (see below). This ratio was called the time-resolved magnetic field effect (TRMFE).

As an example of experimental setup for TRMFE studies, Figure 3 presents a block diagram of an X-ray fluorimeter designed at the same Institute, Siberian Branch of the Russian Academy of Sciences. This instrument was used to obtain many of the results discussed below. The electron gun was also designed at the Institute of Chemical Kinetics and Combustion, Siberian Branch of the Russian Academy of Sciences and is used to generate X-ray pulses in the ~ 20 keV energy range. X-Ray radiation incident on the sample placed between the poles of an electromagnet causes fluorescence, which passes through the light guide and light filter to the photomultiplier

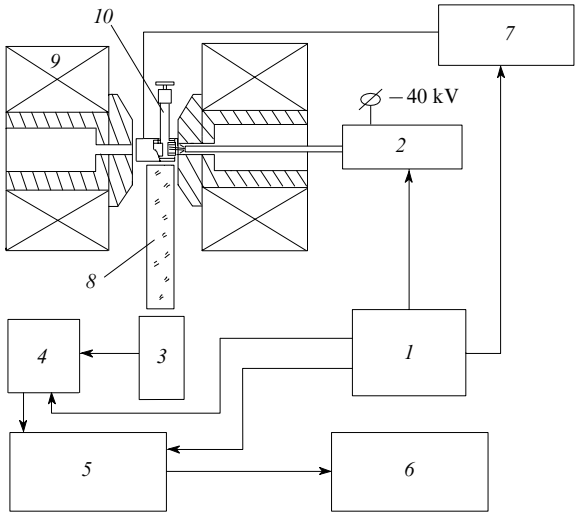


Figure 3. Blok diagram of a nanosecond X-ray fluorimeter.[49] Synchronisation and control unit (*1*), electron gun (*2*), fluorescence detection unit (*3*), converter of time intervals (*4*), multichannel analyser (*5*) coupled with a computer (*6*), magnetic field and temperature control unit (*7*), light guide (*8*), electromagnet (*9*), and sample (*10*).

and the fluorescence detection unit. The fluorimeter makes it possible to detect the kinetics of radiofluorescence on the time scale from 10 to 10^4 ns at the magnetic field induction ranging from 0 to 1.1 T and provides temperature stabilization in the 223 – 353 K range.

4. First observations of quantum beats

Quantum beats due to hyperfine coupling were first observed by Klein and Voltz[26, 27] in 1976 and independently by Brocklehurst.[28, 29] Klein and Voltz[26, 27] measured the kinetics of recombination fluorescence induced by irradiating a cyclohexane solution of a dye [2,5-bis(4-butylphenyl)-1,3,4-oxadiazole, bPPD] with fast electrons in magnetic field by the single photon counting technique at times up to 700 ns. Having plotted the TRMFE curve, the authors revealed a kink. The nonmonotonic character of the TRMFE curve was associated with magnetic-field-dependent singlet – triplet transitions in the secondary radical ion pairs $bPPD^{+\bullet}/bPPD^{-\bullet}$. These transitions determine the multiplicity of the RP at the instant of recombination and, as a consequence, the multiplicity of the recombination product, *i.e.*, an excited bPPD molecule. As a result, fluorescence due to emission of singlet-excited molecules of this dye is modulated, the modulation frequencies being equal to the singlet – triplet transition frequencies.

Brocklehurst reported similar experiments with other luminophores (*p*-terphenyl and biphenyl) in various non-polar solvents.[28, 29] Researchers from both groups used radicals with complex hyperfine structures characterised by a number of different HFC constants. As a result the TRMFE curves exhibited a single peak of oscillations (Fig. 4), thus providing a little information on the phenomenon under study.[11] The authors of the pioneering and subsequent studies (see a review[11]) clearly demonstrated the possibility of observation of the spin evolution in RPs using the TRMFE technique.

Studies reported by Anisimov *et al.*[30, 31] in 1983 gave a new impetus to the development of the method of quantum beats in recombination fluorescence. Anisimov *et al.* observed a number of quantum beat peaks in the kinetics of recombination luminescence of the solutions of tetramethylethylene

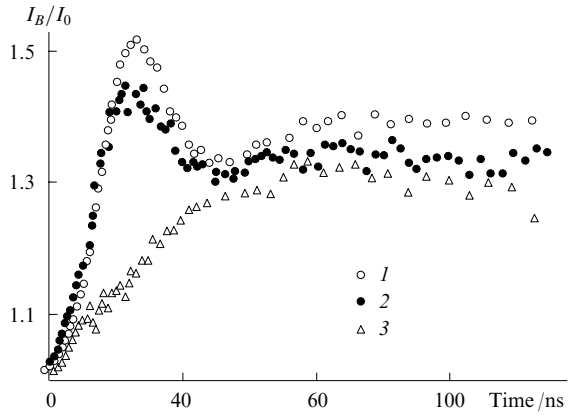


Figure 4. Magnetic field effect (B = 100 mT) in recombination fluorescence for squalane solutions of *p*-terphenyl (curves *1* and *2*) and *p*-terphenyl-d_{14} (curve *3*). Solute concentration: 5 mmol litre^{-1} (*1*) and 1 mmol litre^{-1} (*2*, *3*).[11]

(2,3-dimethylbut-2-ene) and *p*-terphenyl-d_{14} in *trans*-decalin, *cis*-decalin, squalane and pentadecane in strong (Fig. 5) and zero magnetic field.

Tetramethylethylene chosen as hole scavenger forms a radical cation containing twelve equivalent protons. Therefore, the pattern of quantum beats in a strong magnetic field is formed by oscillations with the multiple frequencies and looks quite simple. Similar results were obtained [30, 31] in studies of a solution of durene (its radical cation also contains twelve equivalent protons) and *p*-terphenyl-d_{14} in *trans*-decalin. Both the shape and period of oscillations corresponded to the theoretically predicted ones, but the amplitude of beats observed in the experiments was much smaller than it follows from theory.

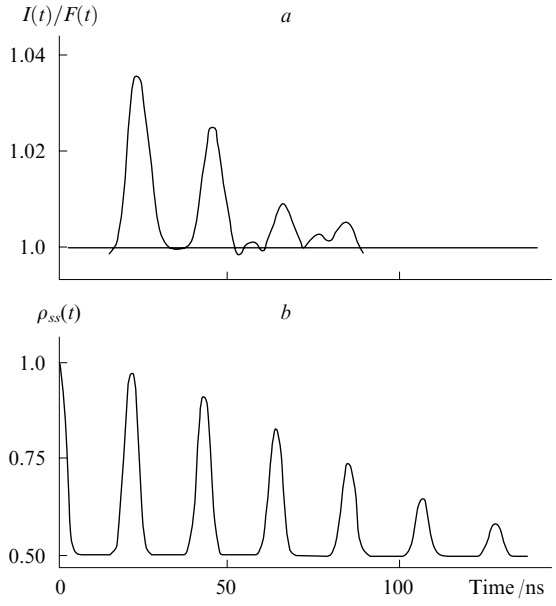


Figure 5. Quantum beats in recombination fluorescence of tetramethylethylene and *p*-terphenyl-d_{14} solutions in *trans*-decalin in a magnetic field of 0.33 T, detected as the ratio of the fluorescence kinetics to the smooth function $F(t)$ simulating the recombination kinetics (*a*) and theoretical curve for the singlet state population of the RP (*b*).[30]

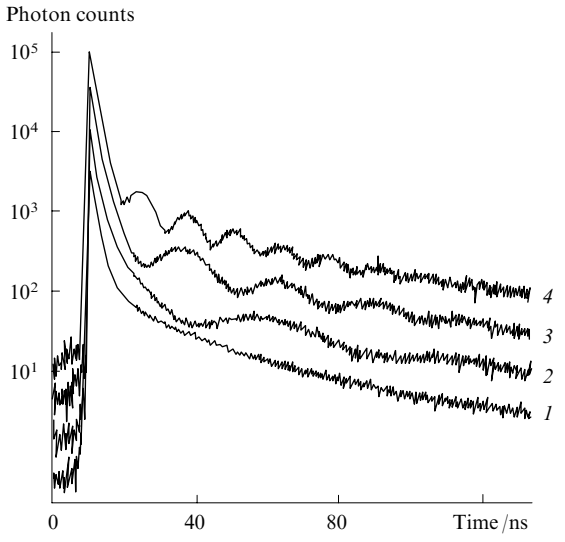


Figure 6. Recombination fluorescence kinetics of a isooctane solution of mixture of *p*-terphenyl-d_{14} (1 mmol litre^{-1}) with diphenyl sulfide-d_{10} (30 mmol litre^{-1}) in magnetic field of 0.017 (*1*), 0.24 (*2*), 0.48 (*3*) and 0.96 T (*4*).[36] For clarity, the curves are arbitrarily shifted along the Y axis.

Researchers from this group also detected quantum beats due to the *g*-factor differences between radicals in the solutions of diphenyl sulfide-d_{10} and *p*-terphenyl-d_{14} in various solvents (Fig. 6).[32, 33, 35–38]

The (diphenyl sulfide-d_{10})$^{+\bullet}$ and (*p*-terphenyl-d_{14})$^{-\bullet}$ radical ions produced in such solutions are characterised by negligible HFC constants and significantly different *g*-factors. The amplitude of beats was found to be much larger compared to the results of the earlier studies.[30, 31] In this case the frequency of beats is proportional to the induction of external magnetic field.

III. Theory of quantum beats in recombination luminescence of spin-correlated radical ion pairs

Theory of quantum beats in the spin states of radical pairs has been well developed for isotropic HFC.[2] No analytical solution for the general case of arbitrary magnitudes of HFC constants and magnetic fields is available. However, most of experimental data can be approximately described using analytical solutions derived for some particular cases. These analytical results are of paramount value because the computational cost of the available algorithns of numerical solution to this problem is very high. This strongly complicates calculations and makes them of limited use in simulating experimental curves.

The possibility of manifestation of singlet–triplet transitions in recombination of radical pairs was first reported by Brocklehurst in 1969.[67] He analysed a radiation-chemical process of geminate recombination of an electron (or radical anion) with the parent radical cation and assumed that in this case the S–T transitions in the pair can affect the product ratio and that these transitions are induced by paramagnetic relaxation of electron spins. In the mid-1970s, interest in the singlet–triplet evolution in RPs increased after carrying out the pioneering experiments on observation of recombination fluorescence.[26, 27, 43] At that time, Brocklehurst [44, 68] and Schulten and Wolynes [69] calculated the effect of HFC on the singlet–triplet transitions for some particular cases. Further development of the theory of singlet–triplet evolution is associated with the studies by Salikhov, his followers and colleagues who succeeded in deriving analytical solutions for

a broader range of hyperfine interactions (key results were reported in a monograph [2]). Some practically valuable relationships were derived recently.[42, 70–72]

A salient feature of radical ion pairs produced in solution upon the action of a pulse of ionising radiation is that only a fraction of them is in the spin-correlated singlet state. Theoretical models usually assume that recombination of both correlated and uncorrelated pairs obeys the same kinetic law and that fluorescence of the excited molecules of recombination products occurs instantaneously. Then, the experimentally observed kinetics of the fall-off of recombination fluorescence intensity $I(t)$ is given by [42, 50, 51]

$$I(t) \propto F(t)\left[\theta\rho_{ss}(t) + \frac{1}{4}(1-\theta)\right].$$

Here $F(t)$ is the rate of pair recombination, θ is the fraction of singlet-correlated pairs, $\rho_{ss}(t)$ is the temporal dependence of the singlet state population of the spin-correlated pair, which is determined by both dynamic spin processes and the spin relaxation and strongly depends on the strength of the applied magnetic field. The second term in the square brackets includes the contribution of the singlet component of spin-uncorrelated pairs to fluorescence.

As mentioned above, the $I_B(t)/I_0(t)$ ratio (time-resolved magnetic field effect) is more convenient for analysis. This ratio is independent of the function $F(t)$, being determined only by the evolution of the spin state.

$$\frac{I_B(t)}{I_0(t)} = \frac{\theta\rho_{ss}^B(t) + 1/4(1-\theta)}{\theta\rho_{ss}^0(t) + 1/4(1-\theta)} \tag{7}$$

Here the superscripts 'B' and '0' indicate that the system is in external nonzero and zero magnetic field, respectively. This simplifies the situation and allows the spectral parameters to be determined by fitting relation (7) to the experimentally measured TRMFE using the singlet state populations $\rho_{ss}(t)$ calculated in the framework of a particular model for hyperfine coupling in radical ions of the pair.

When calculating the singlet state population $\rho_{ss}(t)$, one should allow for the fact that the initial spin state of the radical pair is correlated (sometimes, it is called 'entangled' state), *i.e.*, the corresponding density matrix cannot be represented as the product of the density matrices of subsystems. This means that, generally, it is impossible to write the solution as the product of the functions, each of them corresponding to a single radical. At the same time the absence of interactions between electron spins of radicals in the pair, which is characteristic of the examples considered in this review, simplifies the solution and it can be written in the form reported by Schulten and Wolynes,[69]

$$\rho_{ss}(t) = \frac{1}{4} + \sum_{i,k} T_{ik}^{(1)}(t)T_{ik}^{(2)}(t), \tag{8}$$

where $i,k = \{x,y,z\}$, and the components of the correlation tensor are

$$T_{ik}^{(1)}(t) = \left\langle Tr_e\left\{\hat{S}_{1i}(t)\hat{S}_{1k}(0)\right\}\right\rangle, \tag{9}$$

$$T_{ik}^{(2)}(t) = \left\langle Tr_e\left\{\hat{S}_{2i}(t)\hat{S}_{2k}(0)\right\}\right\rangle.$$

Here $\hat{S}(t)$ are the operators of the electron spins of the radicals in the Heisenberg representation. The superscripts '1' and '2' in the tensors and the subscripts '1' and '2' in the spin operators correspond to different radicals in the RP; Tr_e denotes the trace over electron spin variables and the angle brackets denote the averaging over projections of the magnetic nuclei. Equation (8) makes it possible to obtain the solution to the problem of the spin evolution of the RP using the components of the correlation tensor, each of them depending only on the Hamiltonian of one radical.

As mentioned above, there is no general analytical solution for the components of the correlation tensor at arbitrary HFC in each radical in the RP and arbitrary magnetic field. Now we will consider some particular cases of isotropic HFC with the known analytical solutions.

1. One magnetic nucleus or equal HFC constants for all magnetic nuclei in arbitrary external magnetic field

The results for the case of HFC with one magnetic nucleus were reported earlier;[2, 68] the corresponding expressions written in a more convenient form [70] are as follows:

$$T_{xx} = T_{yy} = \frac{1}{2}\mathrm{Re}(h(t)), \tag{10}$$

$$T_{xy} = -T_{yx} = \frac{1}{2}\mathrm{Im}(h(t)),$$

$$T_{zz} = \frac{1}{2}g(t),$$

where

$$g(t) = 1 - \frac{a^2}{2I+1}\sum_{m=-I}^{I}\frac{I(I+1)-m(m+1)}{(2R_m)^2}\left[1-\cos(2R_m t)\right],$$

$$h(t) = \frac{1}{4(2I+1)}\sum_{m=-I}^{I}\left[(1+D_m)e^{\mathrm{i}R_m t} + (1-D_m)e^{-\mathrm{i}R_m t}\right]\times$$
$$\times\left[(1+D_{m-1})e^{\mathrm{i}R_{m-1}t} + (1-D_{m-1})e^{-\mathrm{i}R_{m-1}t}\right] \tag{11}$$

and

$$2R_m = \sqrt{\omega_0^2 + a\omega_0(2m+1) + a^2\left(I+\frac{1}{2}\right)^2},$$

$$D_m = \frac{\omega_0 + a(m+1/2)}{2R_m}.$$

In the last two relationships $\omega_0 = g\beta B/\hbar$ is the Larmor precession frequency of electron spin in external field, g is the g-factor of the radical, β is the Bohr magneton, B is the magnetic field induction, $\hbar$ is the Planck constant, a is the isotropic HFC constant expressed in circular frequency units, m is the nuclear spin projection on the magnetic field direction and I is the spin of the magnetic nucleus in the radical.

This result can also be used in the case of a group of nuclei with equal HFC constants. Here, expressions (10) and (11) should be averaged over the spin I treated as the total spin of the magnetic nuclei. The weight P_I of each I value can be found by adding the spins of magnetic nuclei characterised by equal HFC constants. In particular, for n nuclei with the spin 1/2 (see Ref. 42) one has

$$P_{n,I} = \frac{(2I+1)^2 n!}{2^n[(n/2)-I]![(n/2)+I+1]!}.$$

In weak magnetic fields, a specific situation of weak HFC in one and strong HFC in the other radical in the pair is also possible (for both radicals the HFC constant is compared to the induction of external magnetic field). It was theoretically predicted and experimentally confirmed that in this case quantum beats at a frequency similar to the frequency of Larmor precession of electron spin manifest themselves in recombination fluorescence.[64, 65]

2. The singlet state population of a radical pair in zero magnetic field

In zero external magnetic field we deal with the diagonal tensor (9) having equal principal values. Therefore, in zero magnetic field one gets

$$\rho_{ss}^{0}(t) = \frac{1}{4} + 3T_{zz}^{(1)}(t)T_{zz}^{(2)}(t). \tag{12}$$

In the presence of a HFC with only one nucleus with the spin I (HFC constant a) in zero magnetic field one has [2]

$$T_{zz}(t) = \frac{3 + 4I(I+1) + 8I(I+1)\cos[a(I+1/2)t]}{6(2I+1)^2}. \tag{13}$$

In the case of several magnetic nuclei with equal HFC constants, expression (13) should be averaged over the total nuclear spin I. For instance, the expression for a group of n nuclei with the spin 1/2 and equal HFC constants a, has the form [42]

$$T_{zz}(t) = \frac{1}{6}\left[\frac{n+3}{n+1} + \frac{2n(n+2)}{n+1}\left(\cos\frac{at}{2}\right)^{n+1} - 2n\left(\cos\frac{at}{2}\right)^{n-1}\right]. \tag{14}$$

Schulten and Wolynes derived [69] an approximate solution for the case of a large number of magnetic nuclei characterised by small, but not necessarily equal, HFC constants; this corresponds to an unresolved EPR spectrum of a radical. To allow for zero magnetic field in this approximation, expression (12) should be written using the quantity

$$T_{zz} = \frac{1}{6}\left[1 + 2C(\sigma t)\right],$$

where

$$C(x) = \left(1 - x^2\right)e^{-0.5x^2},$$

and the parameter σ^2 is the second moment of the EPR spectrum of the radical:

$$\sigma^2 = \frac{1}{3}\sum_n a_n^2 I_n(I_n + 1). \tag{15}$$

An approximate solution to the problem of the spin evolution in a singlet-correlated pair of noninteracting radicals in zero magnetic field was derived for the case where one nucleus (or a group of equivalent nuclei) in the radical is involved in isotropic HFC characterised by a large HFC constant and other nuclei have relatively small (not necessary equal) HFC constants.[71] In EPR and NMR spectroscopy this is called 'inhomogeneous line broadening'. Simulation [71] showed that this type of broadening affects the spin dynamics similarly to phase relaxation.

An analytical solution for $T_{zz}(t)$ in the case of isotropic HFC with two groups of equivalent nuclei in zero magnetic field is also available.[72] In the two last-named cases, the solutions are cumbersome, so we have to address the reader to the original studies.[71, 72]

3. The singlet state population of a radical pair in a strong magnetic field

Considering the case of a strong magnetic field whose strength much exceeds the HFC constants of the radicals in the RP, one can use the high-field approximation[2] to simplify the Hamiltonian of the RP. Here, assuming an isotropic HFC tensor and g-tensor, expression (8) takes the form

$$\rho_{ss}(t) = \frac{1}{2} + \frac{1}{2}\cos\left[(\omega_{01} - \omega_{02})t\right]G_1(t)G_2(t), \tag{16}$$

where ω_{01} and ω_{02} are the frequencies of Larmor precession of electron spins in the magnetic field and the functions $G(t)$ are determined by the HFC constants (a_n) and the spins of the magnetic nuclei (I_n) in each radical in the RP

$$G(t) = \prod_n \left\{\frac{1}{(2I_n+1)}\frac{\sin\left[a_n(2I_n+1)t/2\right]}{\sin(a_n t/2)}\right\}. \tag{17}$$

Here the subscript n enumerates the magnetic nuclei.

The solution (16), (17) was first reported by Brocklehurst [68] in the form of a relation for the singlet state population at particular I values. In a particular case where one radical contains n_1 and the other radical contains n_2 equivalent nuclei with the spin $I = 1/2$ and the HFC constants a_1 and a_2, respectively, one gets

$$\rho_{ss}(t) = \frac{1}{2} + \frac{1}{2}\cos\left[(\omega_{01} - \omega_{02})t\right]\left(\cos\frac{a_1 t}{2}\right)^{n_1}\left(\cos\frac{a_2 t}{2}\right)^{n_2}.$$

In the quasi-classical approximation,[69] which is valid for many magnetic nuclei having small HFC constants, the functions (17) take the form

$$G(t) = e^{-(\sigma^2 t^2)/2},$$

where the second moment of the EPR spectrum σ^2 is given by Eqn (15).

4. Taking into account the effect of paramagnetic relaxation

The effect of paramagnetic relaxation on the singlet state population of RPs in a strong and zero magnetic field was also included as follows.[13, 17, 42, 45, 46, 50–61] Let $\rho'_{ss}(t)$ be the singlet state population calculated ignoring paramagnetic relaxation. The singlet state population with allowance for relaxation in a strong magnetic field is given by

$$\rho_{ss}(t) = \frac{1}{4} + \frac{1}{4}e^{-t/T_1} + e^{-t/T_2}\left(\rho'_{ss}(t) - \frac{1}{2}\right), \tag{18}$$

and the corresponding expression for zero magnetic field has the form

$$\rho_{ss}(t) = \frac{1}{4} + e^{-t/T_0}\left(\rho'_{ss}(t) - \frac{1}{4}\right), \tag{19}$$

where T_1 and T_2 are, respectively, the longitudinal and transverse paramagnetic relaxation times in the strong magnetic field and T_0 is the transverse paramagnetic relaxation time in zero magnetic field.

Although some theoretical background substantiating relations (18) and (19) is available,[5, 11, 45] one must admit that these equations are based on semiempirical considerations only. Namely, in the strong magnetic field the transverse relaxation mixes the singlet state of the RP with only one of the three triplet states in which the spin projection on the magnetic field direction is zero. This means that the asymptotic $\rho_{ss}(t)$ value in the presence of transverse relaxation is 1/2. In Eqn (18), this is included by the exponent e^{-t/T_2}. At the same time longitudinal relaxation equilibrates the populations of the singlet state and all the three triplet states [see the exponent e^{-t/T_1} in Eqn (18)]. In zero magnetic field there is no preferred axis and the rates of longitudinal and transverse relaxation should be equal to each other.

This approach usually provides a satisfactory description of experimental results using a minimum number of relaxation rate parameters, namely, two and one for the case of a strong and zero magnetic field, respectively. At the same time this may appear to be insufficient for rigorous treatment of a particular physical mechanism of paramagnetic relaxation.[73]

IV. Spectroscopy of quantum beats in radical pairs

Spectroscopic information on the partners of a radical pair extracted by the method of quantum beats is similar to that obtained in EPR studies. The key advantages of the title method are much higher sensitivity and the possibility of detecting species characterised by the lifetimes of up to a few nanoseconds. Development of this technique made it possible to study short-lived radical ion species in liquid solutions at ambient temperatures.

1. Determination of hyperfine coupling constants and *g*-factors of radical ions

The simple TRMFE curves for the case of hyperfine coupling with a number of equivalent protons in one partner of the radical pair were analysed.[42] It was shown that in this case quantum beats manifest themselves as a sequence of peaks in the TRMFE curve. The position of the first peak on the time scale is determined by the second moment of the EPR spectrum of this radical. For even number of protons, the next peak is more intense and its position is determined by the HFC constant. If the number of protons is odd, a trough occurs instead of the peak. Then the beats show a periodic damping pattern due to relaxation. These predictions were checked in the same study[42] taking radical cations of nine compounds (alkanes, alkenes and aromatics) with equivalent protons. The *p*-terphenyl-d_{14} radical anion, whose HFC constants are small and make a negligible contribution to the spin evolution of the pair, served as the geminate partner. Figure 7 presents some examples of the TRMFE curves. The HFC constants determined from the instants corresponding to the appearance of the second peak are listed in Table 1. It should be noted that the obtained HFC constants coincided with the published data measured by other methods.

The possibility of determining both the HFC constants and the *g*-factor differences between radical ions was demonstrated[52] taking the hexamethylethane (2,2,3,3-tetramethylbutane) radical cation as an example. The EPR spectrum of this species is governed by isotropic HFC with eighteen equivalent protons. The HFC constant was calculated from positions of peaks in the TRMFE curve, and the *g*-factor difference between the $(\text{hexamethylethane})^{+\bullet}$ and $(p\text{-terphenyl-}d_{14})^{-\bullet}$ radical ions was determined from analysis of the dependence of the shape of the TRMFE curve (Fig. 8) on the magnetic field strength. These results coincided with the data obtained in the same study by the optically detected EPR (OD EPR) technique and with the published data.

Table 1. HFC constants (*a*) for radical cations of various electron donors in nonpolar solutions measured by quantum beats technique.

Donor	*a* /mT [a]	Ref.
cis-Decalin	4.5 (4H)	42
9,10-Octalin	2.4 (8H)	42
Tetramethylethylene	1.6 (12H)	42
Octamethyl-1,4-cyclohexadiene	0.7 (12H)	42
p-Xylene	1.7 (6H)	42
p-Diethylbenzene	1.7 (4H)	42
1,2,4,5-Tetramethylbenzene	1.0 (12H)	42
Hexamethylbenzene	0.6 (18H)	42
Hexamethylethane	1.24 (18H)	52
2,3-Dimethylbutane	1.66 (12H)	72
	0.65 (2H)	72
2,2,6,6-Tetramethylpiperidine	−1.85 (1H)	72
	1.78 (1N)	72
Diisopropylamine	2.1 (1N)	72
	2.1 (2H)	72
	−2.4 (2H)	72
2,2,3-Trimethylbutane	1.24 (9H)	66
	1.55 (6H)	66
2,2,4-Trimethylpentane	1.3 (10H)	66
	0.37 (6H)	66
2,2-Dimethylpentane	1.33 (11H)	66
	0.39 (3H)	66
2,2,4,4,6,8,8-Heptamethylnonane	$\sigma = 1.6$ [b]	66

[a] Figures in parentheses denote the number and types of nuclei. [b] Parameter of the second moment of the EPR spectrum of the radical cation.

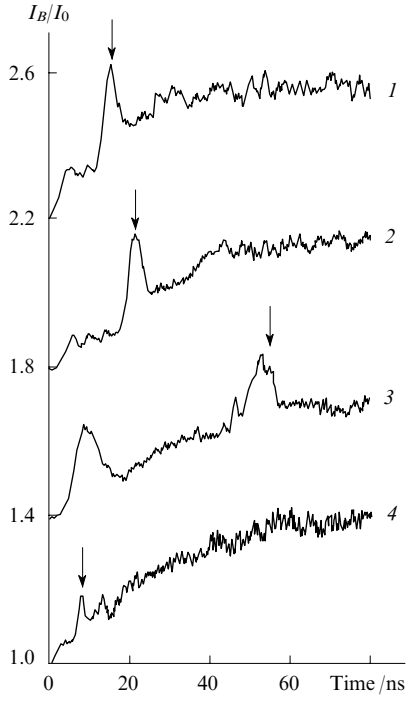


Figure 7. TRMFE curves for dilute cyclohexane solutions of mixtures of *p*-terphenyl-d_{14} with 9,10-octalin (*1*), tetramethylethylene (*2*), octamethylcyclohexa-1,4-diene (*3*) and *cis*-decalin (*4*).[42]
The arrows show the theoretical positions of the second (main) peak.

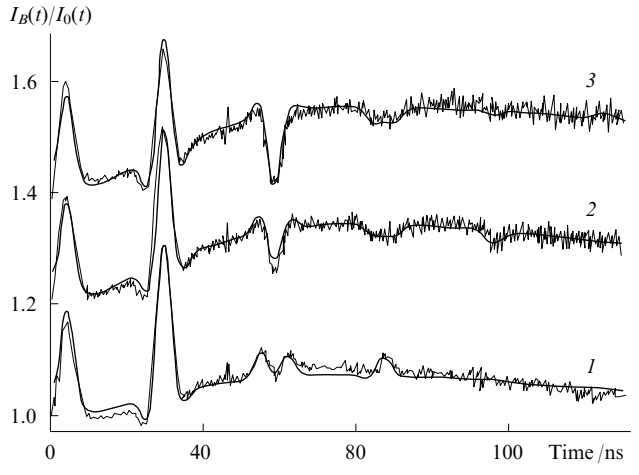
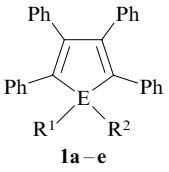


Figure 8. TRMFE curves of dilute n-hexane solutions of mixture of hexamethylethane with *p*-terphenyl-d_{14} in magnetic field of 0.1 (*1*), 0.5 (*2*) and 0.7 T (*3*).[52]
Smooth solid curves represent the results of simulation of experimental data.

The TRMFE method was used to study radical anions of 1,2,3,4-tetraphenylcyclopenta-1,3-diene (**1a**) and its heteroorganic analogues containing silicon (**1b**) and germanium (**1c**–**e**) in n-decane solutions.[50, 51]



1a–**e**

E = C, $R^1 = R^2$ = H (**a**);
E = Si, $R^1 = R^2$ = H (**b**);
E = Ge: $R^1 = R^2$ = H (**c**);
$R^1 = R^2$ = Cl (**d**);
R^1 = Me, R^2 = Cl (**e**).

Simulation of experimental curves (Fig. 9) gave the following HFC constants:

Compound **1**	a /mT
a	2.50 ± 0.04 (2H)
b	1.56 ± 0.03 (2H)
c	1.50 ± 0.03 (2H)
d	0.7 ± 0.1 (2Cl)
e	1.14 ± 0.1 (Cl)

Reliable detection of this type of radical anions by the TRMFE method indicates that their lifetimes in solution are at least of the order of tens of nanoseconds. This is of great importance for chemistry of such compounds, because attempts to detect these species (except for radical anion **1a**) by other methods failed and the possibility of their formation in solutions cast some doubts.

The contributions of each radical in the pair to the spin evolution [see Eqns (14) and (16)] can be separated.[53] Figure 10 shows the TRMFE curves obtained for an n-octane solution of mixture of hexamethylethane (0.1 mol litre^{-1}) with tetraphenylcyclopentadiene (3×10^{-4} mol litre^{-1}) at a magnetic field induction of 0.1 and 0.7 T at room temperature. The spin evolution is determined by the hyperfine coupling in the (hexamethylethane)$^{+\bullet}$/(tetraphenylcyclopentadiene)$^{-\bullet}$ pair. The former species is involved in HFC with eighteen equivalent protons (HFC constant a_1 = 1.24 mT), while the latter has two equivalent protons (HFC constant a_2 = 2.46 mT). The smooth curves in Fig. 10 represent the results of approximation of experimental data by a relevant model. Although the pattern of beats is more complicated, experimental data are well described by the theory.

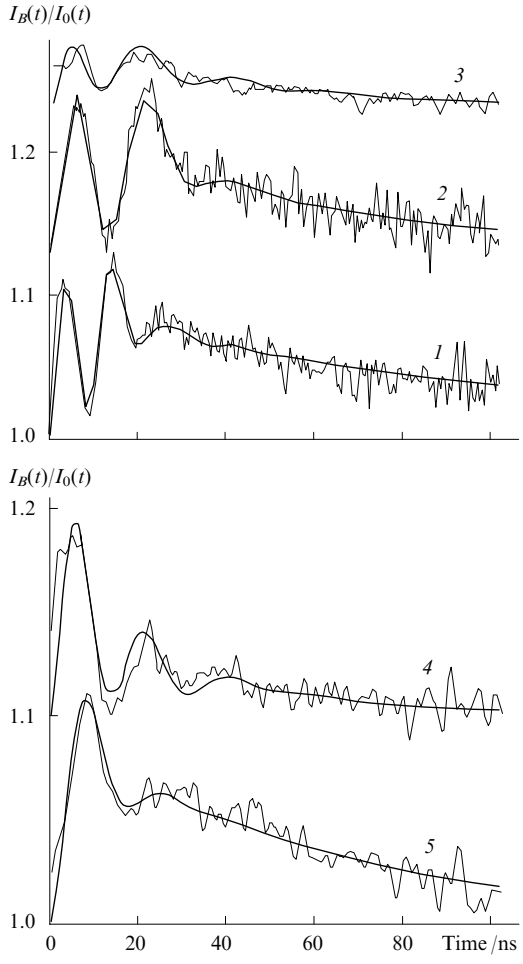


Figure 9. TRMFE curves of solutions of 1,2,3,4-tetraphenylcyclopenta-1,3-diene (*1*) and its heteroorganic analogues **1b** (*2*) and **1c**–**e** (*3*–*5*) in n-decane.[51]
Smooth solid curves represent the results of simulation of experimental data.

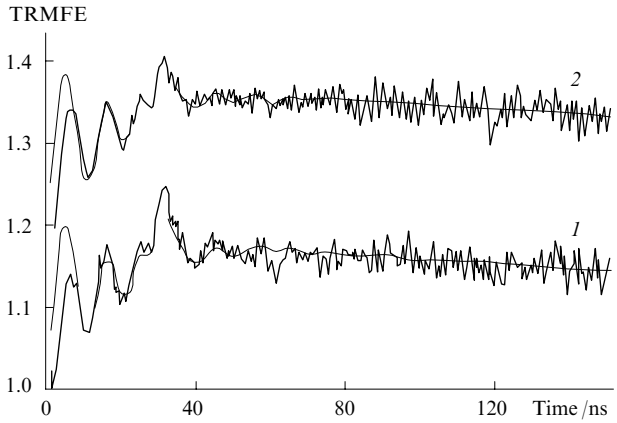


Figure 10. TRMFE curves of solutions of hexamethylethane and tetraphenylcyclopentadiene in n-octane [B = 0.1 (*1*) and 0.7 T (*2*)].[53]
Smooth solid curves represent the results of simulation of experimental data.

The 2,3-dimethylbutane, 2,2,4,4-tetramethylpiperidine and diisopropylamine radical cations containing two groups of magnetically equivalent nuclei were studied.[72] In addition to the calculation of absolute values of the HFC constants, the authors of this study confirmed the theoretically predicted possibility of determining the signs of the HFC constants for groups of nuclei. In Fig. 11 we present the experimental curve

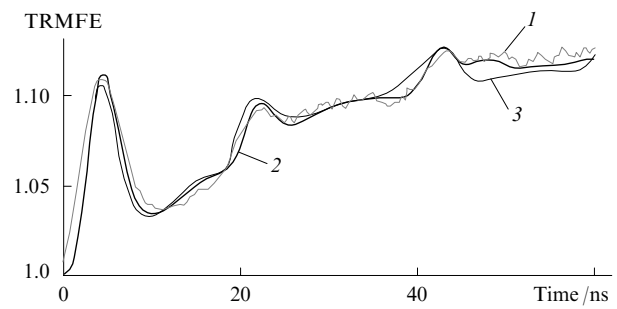


Figure 11. TRMFE curve for an n-hexane solution of mixture of 2,3-dimethylbutane with *p*-terphenyl-d_{14} (*1*) and best fits of experimental data using a model with the HFC constants a (12H) and a (2H) of the same sign (*2*) and of different signs (*3*).[72]

of TRMFE due to hyperfine coupling in the 2,3-dimethylbutane radical cation. The best approximation of experimental data with the '12H + 2H' model gave the same signs of the HFC constants for these groups of protons, which was confirmed by quantum chemical calculations. Calculations with the HFC constants of different sign led to poorer agreement with the experiments.

Radical cations of branched alkanes and their heteroorganic analogues Me_4E and Me_3EEMe_3 (E = C, Si, Ge, Sn) in hexane were studied by the TRMFE method [54] and the *g*-factors and HFC constants of the heteroorganic radical cations were obtained. Fast degenerate electron exchange (DEE) was observed in the Me_4E compounds, whereas this was not observed in the Me_3EEMe_3 compounds. It was found that, in contrast to the alkane radical cations, the heteroorganic ones are characterised by short phase relaxation time of the order of 10 ns. The authors believed that a large contribution to relaxation comes from the spin-rotational interaction and degenerate electron exchange. The last-mentioned mechanism is particularly efficient due to a considerable proportion of magnetic isotopes ^{29}Si, ^{73}Ge, ^{117}Sn and ^{119}Sn.

A number of radical cations of branched alkanes were studied.[66] The formation of such species upon radiolysis of solutions was confirmed and their HFC constants were also determined (see Table 1).

2. Studies of fast chemical reactions involving radical ions by the method of time-resolved magnetic field effect

Along with spectroscopic data, monitoring of quantum beats in recombination luminescence makes it possible to obtain spectroscopic data and information on reactions of short-lived radical ions in solutions. The reaction causes changes in the spin Hamiltonian of the pair, which leads to changes in the character of quantum beats and in the shape of the TRMFE curve. In the text below we present some examples of the reactions of electron transfer and degenerate electron exchange in solutions.

To determine the rate of the transfer of the solvent hole (or an electron) to acceptor, the acceptor concentration should not be too high. In this case the secondary pairs are generated not instantaneously and the scatter of the corresponding formation times should cause a decrease in the amplitude and the appearance of phase shifts of quantum beats. By analysing the changes in the TRMFE pattern it is possible to determine the rate constant for charge transfer.

This approach was first employed in measuring the phase shift of the Δg beats as function of the concentration of diphenyl sulfide-d_{10} used as hole trap.[35–38] This dependence was used to determine the rate constant for solvent (isooctane) hole scavenging by the diphenyl sulfide molecule, which was found to be similar to the value corresponding to the diffusion-controlled process.

A study of alkane solutions of 9,10-octalin revealed a rather strong peak of quantum beats due to hyperfine couplings in the 9,10-octalin radical cations even at rather low concentrations of this compound.[46] The large peak amplitude was explained by the contribution of fast non-stationary stage of electron transfer [reaction (4)] from the 9,10-octalin molecule to the primary radical cation and by the fact that the electron-transfer radius exceeds the geometric radius. The electron-transfer radii determined for three n-alkanes from experimental data using the model proposed are 15.1, 13.9 and 10 Å for octane, decane and dodecane, respectively. A decrease in the electron transfer radii for hydrocarbons C_8, C_{10}, C_{12} was associated with the decrease in the ionisation potential difference between the alkane and 9,10-octalin in this series, which is consistent with the predictions based on the Marcus theory.[74]

The degenerate electron exchange

$$D^{+\cdot} + D' \longrightarrow D + (D')^{+\cdot} \qquad (20)$$

between n-alkane, norbornane and tetramethylsilane molecules and their radical cations was studied by the method of quantum beats.[54–57] In EPR spectroscopy, slow degenerate electron exchange causes broadening of spectral lines, whereas fast degenerate electron exchange leads to the exchange narrowing of the spectrum. These changes in the EPR spectra correspond to characteristic features in the TRMFE curves; by simulating such curves one can determine the rate constant for the exchange reaction.

Figure 12 shows the transformation of the TRMFE curves measured in hexane solutions of n-nonane with an increase in the n-nonane concentration from 0.07 to 3 mol litre^{-1} and in neat n-nonane. The shift of the maximum in the MFE curves following an increase in the nonane concentration is due to the narrowing of the EPR spectrum of the nonane radical cation with an increase in the DEE rate [reaction (20)]. This was also confirmed by calculations (smooth lines in Fig. 12). The theoretical curves were obtained using a mathematical model developed by Schulten and Wolynes.[69] Details of simulation were documented.[55]

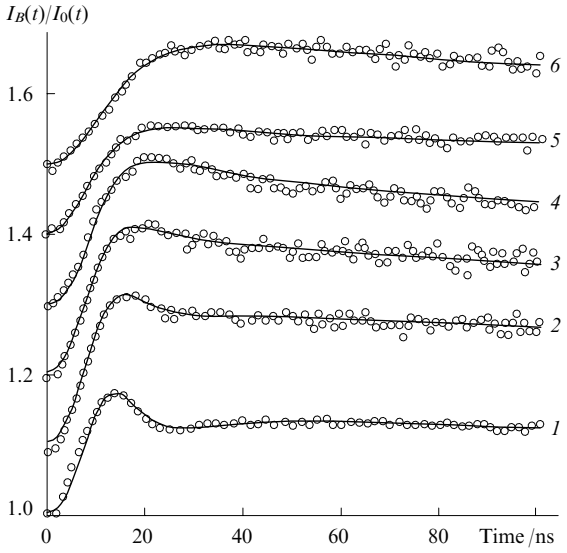


Figure 12. Time-resolved magnetic field effect obtained in hexane solutions of n-nonane at a concentration of 0.07 (*1*), 0.3 (*2*), 0.6 (*3*), 1 (*4*) and 3 mol litre^{-1} (*5*) and in neat n-nonane.[55]
Smooth curves represent the results of simulation using the DEE rates shown in Fig. 13.

The dependence of the DEE rate (τ^{-1}) on the concentration of n-nonane established in Ref. 55 is shown in Fig. 13. Linear character of the rate–concentration plot confirms the bimolecular character of the DEE reaction for n-nonane. n-Alkanes are characterised by much lower DEE rates (two orders of magnitude lower than the rate of diffusion-controlled process). This was explained by the effect of numerous conformations of neutral n-alkane molecules and a rather high activation barrier to electron transfer in the collisional complex between the radical cation and the molecule.[55]

Modulation of the HFC constants due to DEE can induce not only the phase relaxation, but also noticeable spin–lattice relaxation even in a relatively strong magnetic field.[57] The DEE reaction involving the norbornane radical cation containing four equivalent protons with non-negligible HFC constants was studied. The authors reported exact calculations

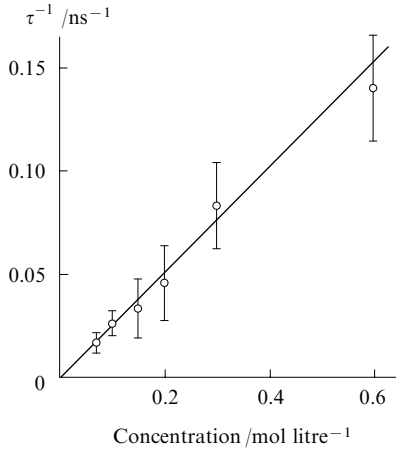


Figure 13. DEE rate for n-nonane radical cation plotted *vs.* n-nonane concentration in hexane solution.[55]
The straight line is the best linear approximation obtained at a rate constant of 2.6×10^8 litre mol^{-1} ns^{-1}.

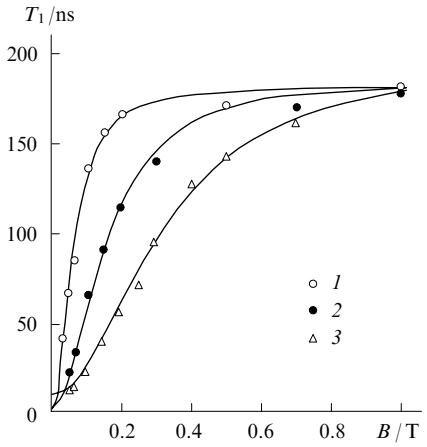


Figure 15. Spin–lattice relaxation time of norbornane radical cation plotted *vs.* magnetic field induction at a norbornane concentration of 0.04 (*1*), 0.2 (*2*) and 0.6 mol litre^{-1} (*3*).[57]
Solid lines represent the results of approximation in the framework of the Redfield theory.

of the evolution of the spin state of the radical pair under DEE conditions. The asymptotic behaviour of the exact dependence of the singlet state population is satisfactorily described by an exponent with a single time parameter, which can be treated as the spin–lattice relaxation time T_1. The T_1 value obtained was similar to that calculated in the framework of the Redfield theory.[75]

Figure 14 shows the TRMFE curves for an n-hexane solution of mixture of norbornane (0.2 mol litre^{-1}) with *p*-terphenyl-d_{14} (30 μmol litre^{-1}) plotted *vs.* magnetic field induction. The fall-off of the TRMFE curves is determined by the rate of spin–lattice relaxation of the norbornane radical cation. Analysis of the dependence of spin–lattice relaxation rate on the magnetic field induction at different norbornane concentrations (Fig. 15) showed that the magnetic field-dependent contribution to relaxation is due to DEE in the norbornane radical cation. The rate constant for DEE was 1.5×10^{10} litre mol^{-1}, which is similar in magnitude to the diffusion-controlled rate constant. The relaxation time of the norbornane radical cation in the strong magnetic field tended to a value of ~180 ns. The nature of the magnetic field independent contribution remains unknown. Probably, it is due to the spin–orbit interaction, as in the case of some cycloalkanes (see below).

The DEE reaction involving the tetramethylsilane (TMS) radical cation in n-hexane was studied.[54] The TRMFE curves obtained for the solution of TMS are shown in Fig. 16. Good agreement between theory and experiment (curve *1*) was attained only assuming that hyperfine coupling in the TMS radical cation is averaged almost to zero due to DEE that occurs under diffusion control.

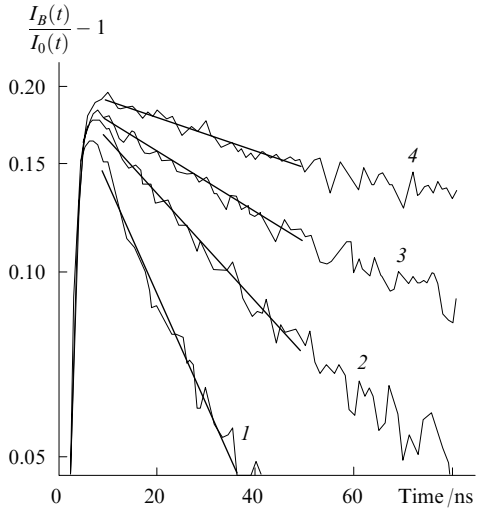


Figure 14. TRMFE curves for an n-hexane solution of mixture of norbornane (0.2 mol litre^{-1}) with *p*-terphenyl-d_{14} (30 μmol litre^{-1}) at a magnetic field induction of 0.05 (*1*), 0.1 (*2*), 0.2 (*3*) and 1 T (*4*).[57]
Straight lines are the exponential approximation of the TRMFE curves in the range of 10 to 50 ns.

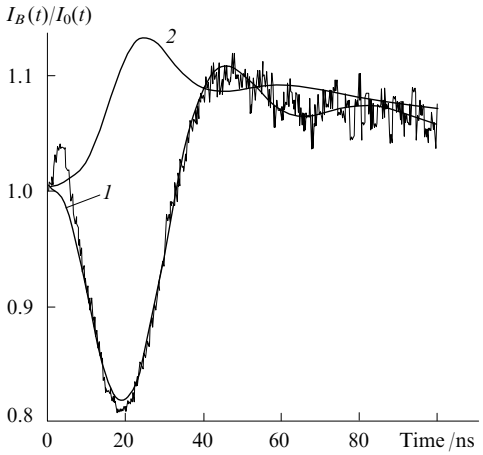


Figure 16. Experimental and theoretical TRMFE curves for a solution of tetramethylsilane and *p*-terphenyl-d_{14} in n-hexane.[54]
Calculated for fast DEE (*1*) and no exchange (*2*).

A radical cation of alicyclic amine, namely, 2,2,4,4-tetramethylpiperidine was studied by the TRMFE and quantum chemistry methods.[58] Based on the changes in the spectra observed upon an increase in the amine concentration and temperature variation, the formation of dimeric radical cations of unusual structure was suggested. A collision between the amine radical cation and the amine molecule is accompanied by proton transfer to the molecule and results in the formation

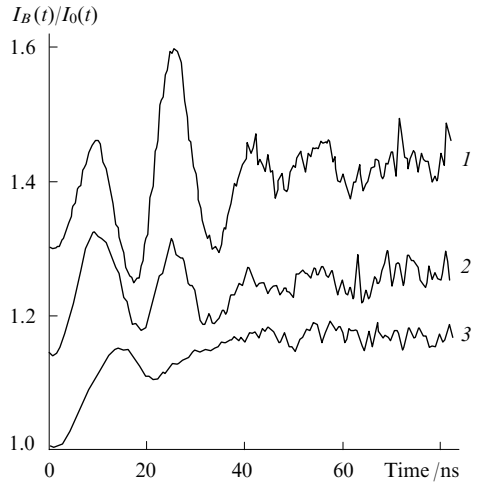


Figure 17. Experimental TRMFE curves obtained for a solution of 2,2,4,4-tetramethylpiperidine and *p*-terphenyl-d_{14} in n-octane ($B = 0.1$ T).[58]
Amine concentration /mmol litre^{-1}: 30 (*1*), 10 (*2*) and 3 (*3*).

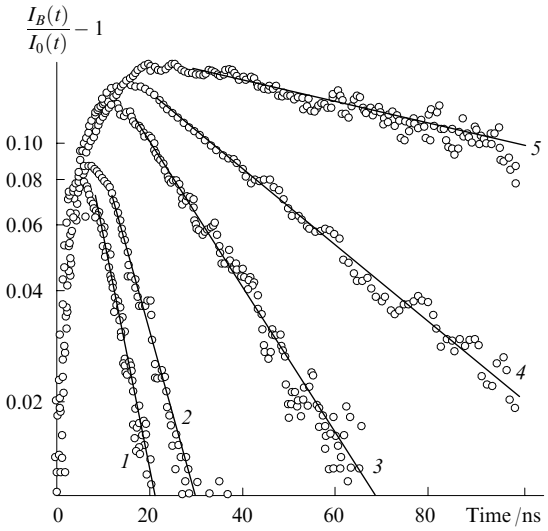


Figure 18. Experimental TRMFE curves ($B = 1$ T) obtained for C_6F_6 solutions in n-hexane in the presence of adamantane (*1*), cyclohexane (*2*), ethylcyclohexane (*3*), methylcyclohexane (*4*) and *cis*-decalin (*5*).[59]
Solid lines represent the results of exponential approximations.

of a rather stable distonic dimer in which the charge and spin are localised on different molecules. The rate constant for dimerisation reaction determined by simulating the changes in the shape of quantum beats pattern with an increase in the amine concentration (Fig. 17) was similar to the diffusion-controlled rate constant.

3. Studies of paramagnetic relaxation in radical ions

The TRMFE technique has unique potential for measuring the spin–lattice relaxation rates of short-lived radical ions in solutions over a wide range of change in the magnetic field induction. Some examples were considered above. Mention can be made of a pioneering study[47] in which the relaxation times of a number of aromatic radical ions (about 1 μs) were measured. Most results can be satisfactorily described in the framework of the relaxation mechanisms known from EPR spectroscopy.

Unusually fast spin–lattice relaxation in the cyclohexane and adamantane radical cations and their alkyl-substituted analogues detected recently by the TRMFE technique appeared to be a surprising exception.[59–61] Figure 18 shows the TRMFE curves obtained for solutions of some cycloalkanes. The exponential decay of the TRMFE curves is determined by the T_1-relaxation. In all cases a three-fold change in the cycloalkane concentration and temperature variation in the 250–320 K range had almost no effect on the rate of T_1-relaxation. The T_1-relaxation times of various cycloalkanes are listed in Table 2.

Using the known data on the EPR spectrum of cyclohexane radical cation and the Redfield theory,[75] it was shown that the relaxation time $T_1 = 9$ ns obtained for the cyclohexane radical cation at a magnetic field induction of 1 T is due to neither modulation of HFC constants or the *g*-tensor anisotropy nor degenerate electron exchange involving the radical cations. Earlier, unusually fast relaxation was observed by EPR spectroscopy in radical anions of some symmetrical aromatic molecules.[76]

Although quantitative theory of unusually fast relaxation has not been developed so far, it is believed[76,77] that the phenomenon can be due to strong spin–orbit interaction in symmetrical radical ions. The unusually fast relaxation in some cycloalkane radical cations provides an explanation for unsuccessful attempts to record their OD EPR spectra.[78]

Table 2. Paramagnetic relaxation times of radical ions generated from corresponding compounds in nonpolar solvents.[59–61]

Compound	T_1 /ns	$T_2 = T_0$ /ns
Hexafluorobenzene [a]	350 ± 15	15 ± 5
cis-Decalin	390 ± 15	10 ± 5
Cyclohexane	9 ± 2	9 ± 2
Methylcyclohexane	57 ± 10	5 ± 2
Ethylcyclohexane	21 ± 3	10 ± 5
Propylcyclohexane	38 ± 4	7 ± 3
Isopropylcyclohexane	280 ± 20	20 ± 5
cis-1,2-Dimethylcyclohexane	280 ± 20	20 ± 5
Adamantane	6.5 ± 1	5 ± 3
1,3-Dimethyladamantane	8.2 ± 1	5 ± 3

[a] A radical anion is produced in this case; all other entries in this Table correspond to radical cations.

4. Manipulation of the spin state of a radical pair

As mentioned above, the character of the spin evolution in a radical pair depends strongly on the external magnetic field. The spin evolution can also be affected by the resonance alternating magnetic field. Pulsed switching-on and(or) switching-off of the magnetic field makes it possible to immediately tamper with the elementary step of RP recombination. The TRMFE technique involving detection of recombination fluorescence permits real-time observation of these effects.

The procedure and results of the first experiments (Fig. 19) on observation of the dynamics of the spin state of a radical ion pair upon fast (~20 ns) switching-off of external magnetic field (initial magnetic field induction 4 mT) were reported.[62] Prior to switching the magnetic field off the system shows a conventional TRMFE pattern determined by the spin evolution in the pair in both zero or nonzero external magnetic field. The fall-off of the TRMFE curves after switching the magnetic field off depends only on the spin evolution in zero field. As should be expected, the fall-off rate is determined by the second moment of the EPR spectrum of radical ions. Deuterated *p*-terphenyl-d_{14} is characterised by a much longer fall-off time compared to non-deuterated *p*-terphenyl.

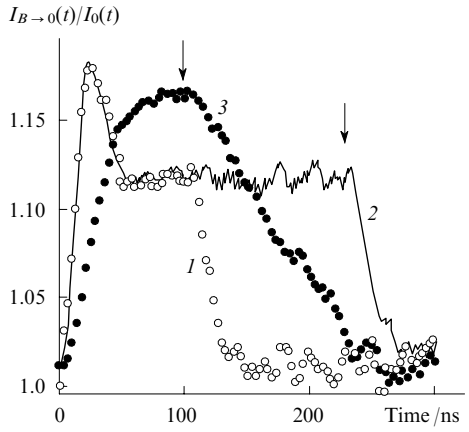


Figure 19. Curves of $I_{B\to 0}(t)/I_0(t)$ ratio obtained for a solution of *p*-terphenyl (10^{-3} mol litre^{-1}) in n-decane at field switching-off delays of 100 (*1*) and 225 ns (*2*) and for a solution of *p*-terphenyl-d_{14} (10^{-3} mol litre^{-1}) in decane at 100-ns delay of the field switching-off (*3*).[62]
The arrows denote the instants of the magnetic field switching-off.

A procedure for control of the course of a spin-dependent reaction using the pulses of alternating resonance magnetic field was studied taking radical ion pair $(C_8H_{18})^{+\bullet}/(p\text{-terphenyl})^{-\bullet}$ as an example.[63] The relative change in the fluorescence intensity (Fig. 20) characterises the change in the singlet state population in the pair in the resonance field. Prior to switching the resonance field off, damping oscillations are observed (see Fig. 20), the oscillation frequency being determined by the amplitude of the magnetic field in the rotating frame.[63] At the instants corresponding to the switching-off of the resonance field (arrowed), the spin state of the pair is 'frozen'. Then, the spin populations are equilibrated at the rate determined by spin–lattice relaxation.

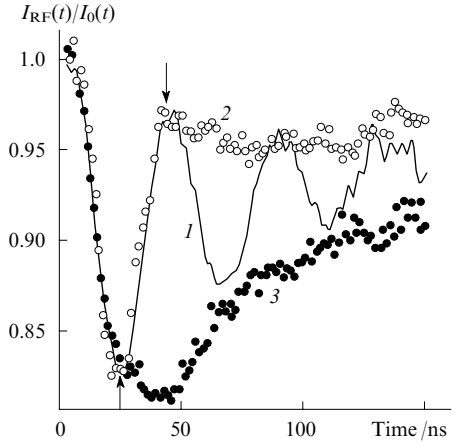


Figure 20. Effect of microwave field, $I_{RF}(t)/I_0(t)$, obtained for a solution of 2,2,4-trimethylpentane and *p*-terphenyl-d_{14} in n-hexane at the resonance UHF field switching-off delays of 300 (*1*), 45 (*2*) and 25 ns (*3*).[63]

5. Radiation chemistry applications

In the examples considered above, ionising radiation only served a convenient instrument of pulsed generation of spin-correlated radical ion pairs. Meanwhile, from the very beginning it was clear that TRMFE studies can provide valuable information on specific features of fast reactions in tracks of ionising particles.

The key role in the development of this avenue of research was played by the studies by Brocklehurst who used the TRMFE technique in recombination luminescence to solve some stubborn problems in radiation chemistry and physics of non-polar solutions. These include the structure of tracks, the origin of superdiffusion mobility of positive charges (solvent holes), the role of excited states in delayed luminescence, the possibility of spin correlation of non-geminate RP in radiation tracks, *etc*. The results obtained by Brocklehurst were summarised in reviews.[11,14] Due to complexity of the problems under study, some of these results are ambiguous. However, in the cited reviews, Brocklehurst touches upon almost all significant details of the processes the radical pairs in radiation tracks are involved in. A thorough study of the dependence of the fraction of the RPs recombining in the spin-correlated state (geminate pairs in the track) on the type and energy of ionising radiation deserves particular attention.

The fraction of geminate radical ion pairs in radiation tracks was determined from the amplitude of quantum beats.[39–41] When different non-polar solutions were irradiated with fast electrons, this quantity was 1.3–2.8 times higher than that found for irradiation with X-rays.[41]

The kinetics of recombination luminescence of non-polar solutions and the magnetic field effect on these kinetics were reported in a study[48] aimed at investigating the formation of radical ion pairs under the action of vacuum ultraviolet; the magnetic field effect observed was used for substantiation of his statement that the primary radical pair is formed from singlet-excited solvent molecule.

6. Quantum beats in laser generation of radical pairs

Laser photolysis undoubtedly belongs to the most widely used methods of pulsed generation of spin-correlated radical pairs and radical ion pairs. However, data on observation of quantum beats in recombination of pairs under laser irradiation are scarce. Most experiments were characterised by low temporal resolution and a complex structure of EPR spectra of the pair partners, which excluded the possibility of obtaining a clearly seen pattern of quantum beats.

Clearly observed beats were reported in a study of time-resolved magnetic field effect on the delayed fluorescence of *N*,*N*,*N*′,*N*′-tetramethyl-1,4-phenylenediamine (TMPD) in alcoholic solutions.[79] Fluorescence was excited by a pulse of a UV laser operating at 308 nm. Irradiation with light resulted in ionisation of TMPD and generation of a spin-correlated pair $(TMPD)^{+\bullet}/e^-$. The spin evolution in this pair caused oscillations at times shorter than 150 ns; at longer times, a magnetic field effect due to triplet–triplet annihilation of excited TMPD molecules was observed.

Real-time observations of manifestations of the spin dynamics of radical pairs were also reported in fast switched magnetic field CIDNP studies.[80–82] A solution irradiated with a laser pulse was placed in a Helmholtz coil that allowed the magnetic field to be switched within the limits of ± 2 mT (switching time 1 ns) with variable delay between the pulse and the switching of magnetic field. Then, the solution was rapidly transferred to the magnet of an NMR spectrometer for CIDNP measurements. In the experiments with radical ion pairs (naphthalene-d_8)$^{+\bullet}$/(1,2-*cis*-dicyanoethylene)$^{-\bullet}$, switching of the magnetic field from 2.3 to 0 mT was followed by oscillations of the CIDNP plotted *vs*. delay time due to the hyperfine interactions in the radical anion. The shapes of these curves (Fig. 21) depend on the concentration of the electron acceptor, which was explained by the effect of degenerate electron exchange.

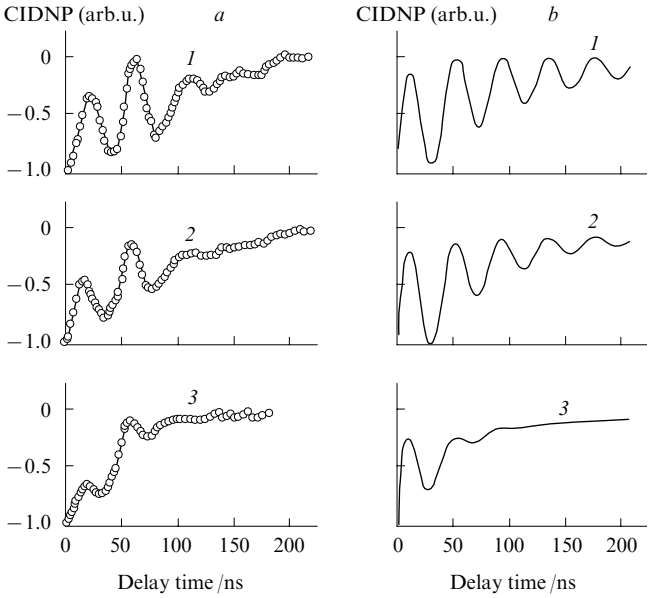


Figure 21. Magnetic field switch CIDNP kinetics observed in photolysis of solutions containing different concentrations of 1,2-*cis*-dicyanoethylene (*a*) and simulation with allowance for DEE (*b*).[81]
Concentration /mmol litre^{-1}: 1 (*1*), 2 (*2*) and 8 (*3*); DEE time /ns: 220 (*1*), 110 (*2*) and 28 (*3*).

V. Conclusion

The method of quantum beats in recombination luminescence proved itself as a powerful tool in the solution studies of short-lived radical ions (lifetimes up to a few nanoseconds). Theoretical foundations of extraction of unique information on these species from experimental data were developed and relevant experimental approaches were implemented. Using the quantum beats technique, one can determine the magnitudes and, in some cases, the signs of the HFC constants of radical ions, the *g*-factors, the paramagnetic relaxation times and the fraction of spin-correlated radical pairs in radiation tracks. The main advantages of the method of quantum beats over conventional EPR spectroscopy consist in the high sensitivity and temporal resolution. The former factor is due to the possibility of carrying out light intensity measurements on the single-photon scale. Therefore, the quantum beats technique makes it possible to study very low concentrations of radical ion pairs (up to about 100 pairs per sample), being enormously more sensitive than EPR spectroscopy. Compared to the OD EPR technique, which is based on the same properties of radical ion pairs, the method of quantum beats provides the possibility of monitoring the course of the chemical reactions involving RPs on the nanosecond time scale.

An apparent limitation of the title method is the necessity of tuning the conditions for a rather high quantum yield of recombination fluorescence and short fluorescence time (it should be shorter than the desired temporal resolution in the experiments). In most cases the radical ions of interest are produced from molecules that do not possess the properties of luminophores. This limitation can be eliminated with ease by choosing an appropriate luminophore as partner (*i.e.*, acceptor of the opposite charge). One can face some difficulties in studies of radical ions in polar solvents. For instance, in this case the energy released in recombination of radical ions may appear to be too low to form an excited luminophore molecule owing to high polarisation energy. These problems are still to be studied, because almost no experiments in polar solvents were carried out as yet.

Prospects for the use of the method of quantum beats are first of all associated with an increase in the number of those radical ions that cannot be studied in solution by other methods due to the short lifetimes. These can be radical ions of heteroorganic or halogen-containing compounds, spin traps, biologically active substances, *etc*.

Yet another promising avenue of research involves the use of laser methods for generation of radical ion pairs. Photoionisation processes attract considerable attention of chemists and physicists and the methods considered above could find wider application. The results of photochemical experiments involving photogeneration of pairs may appear to be simpler to interpret because of the lack of cross-recombination effects typical of radiation tracks. Here, the method of quantum beats could provide additional information on the primary act of formation of radical pairs in solutions upon photoionisation, because many details of this key step remain unknown so far.

This review has been written with financial support from the Chemistry and Materials Science Division of the Russian Academy of Sciences (in the framework of the Basic Research Programme No. 1) and the Federal Programme for State Support of Leading Scientific Schools in the Russian Federation (Grant NSh-5078.2006.3)

References

1. A L Buchachenko, R Z Sagdeev, K M Salikhov *Magnitnye i Spinovye Effekty v Khimicheskikh Reaktsiyakh* (Magnetic and Spin Effects in Chemical Reactions) (Novosibirsk: Nauka, 1978)
2. K M Salikhov, Yu N Molin, R Z Sagdeev, A L Buchachenko *Spin Polarization and Magnetic Effects in Chemical Reactions* (Amsterdam: Elsevier, 1984)
3. *Dynamic Spin Chemistry: Magnetic Controls and Spin Dynamics of Chemical Reactions* (Eds S Nagakura, H Hayashi, T Azumi) (Tokyo: Wiley, Kodansha, 1998)
4. H Hayashi *Introduction to Dynamic Spin Chemistry. Magnetic Field Effects on Chemical and Biochemical Reactions. (World Scientific Lecture and Course Notes in Chemistry)* Vol. 8 (River Edge, NJ: World Sci. Publ., 2004)
5. U E Steiner, T Ulrich *Chem. Rev.* **89** 51 (1989)
6. Y Tanimoto, Y Fujiwara *Handbook of Photochemistry and Photobiology. Inorganic Photochemistry* Vol. 1 (Ed. H S Nalwa) (Stevenson Ranch: American Sci. Publ., 2003) p. 413
7. K Schulten *Advances in Solid State Physics* Vol. 22 (Ed. J Treusch) (Braunschweig: Vieweg, 1982) p. 61
8. N J Turro *Proc. Natl. Acad. Sci. USA* **80** 609 (1983)
9. S G Boxer, C E D Chidsey, M G Roelofs *Annu. Rev. Phys. Chem.* **34** 389 (1983)
10. A L Buchachenko *Usp. Khim.* **62** 1139 (1993) [*Russ. Chem. Rev.* **62** 1073 (1993)]
11. B Brocklehurst *Radiat. Phys. Chem.* **50** 213 (1997)
12. A L Buchachenko *Pure Appl. Chem.* **72** 2243 (2000)
13. Yu N Molin *Bull. Korean Chem. Soc.* **20** 7 (1999)
14. B Brocklehurst *Chem. Soc. Rev.* **31** 301 (2002)
15. S Tero-Kubota, A Katsuki, Y Kobori *J. Photochem. Photobiol., C* **2** 17 (2001)
16. H Murai *J. Photochem. Photobiol., C* **3** 183 (2003)
17. Yu N Molin *Mendeleev Commun.* 85 (2004)
18. C R Timmel, K B Henbest *Philos. Trans. R. Soc. London, Ser. A* **362** 2573 (2004)
19. H Hayashi, Y Sakaguchi *J. Photochem. Photobiol., C* **6** 25 (2005)
20. R Bittl, S Weber *Biochim. Biophys. Acta* **1707** 117 (2005)
21. H Hayashi *J. Chin. Chem. Soc. (Taipei)* **49** 137 (2002)
22. E B Aleksandrov, G I Khvostenko, M P Chaika *Interferentsiya Atomnykh Sostoyanii* (Interference of Atomic States) (Moscow: Nauka, 1991)
23. R T Carter, J R Huber *Chem. Soc. Rev.* **29** 305 (2000)
24. D W Werst *Chem. Phys. Lett.* **251** 315 (1996)
25. L M Bollinger, G E Thomas *Rev. Sci. Instrum.* **32** 1044 (1961)
26. J Klein, R Voltz *Phys. Rev. Lett.* **36** 1214 (1976)
27. J Klein, R Voltz *Can. J. Chem.* **55** 2102 (1977)

28. B Brocklehurst *Chem. Phys. Lett.* **44** 245 (1976)
29. B Brocklehurst *Faraday Discuss. Chem. Soc.* **63** 96 (1977)
30. O A Anisimov, V L Bizyaev, N N Lukzen, V M Grigoryants, Yu N Molin *Chem. Phys. Lett.* **101** 131 (1983)
31. O A Anisimov, V L Bizyaev, N N Lukzen, V M Grigoryants, Yu N Molin *Dokl. Akad. Nauk SSSR* **272** 383 (1983) [a]
32. A V Veselov, V I Melekhov, O A Anisimov, Yu N Molin *Chem. Phys. Lett.* **136** 263 (1987)
33. A V Veselov, V I Melekhov, O A Anisimov, Yu N Molin *Dokl. Akad. Nauk SSSR* **297** 1399 (1987) [a]
34. A V Veselov, V L Bizyaev, V I Melekhov, O A Anisimov, Yu N Molin *Radiat. Phys. Chem.* **34** 567 (1989)
35. V M Grigoryants, B M Tadjikov, O M Usov, Yu N Molin *Dokl. Akad. Nauk* **346** 478 (1996) [a]
36. V M Grigoryants, B M Tadjikov, O M Usov, Yu N Molin *Chem. Phys. Lett.* **246** 392 (1995)
37. O M Usov, D V Stass, B M Tadjikov, Yu N Molin *J. Phys. Chem. A* **101** 7711 (1997)
38. O M Usov, V M Grigoryants, B M Tadjikov, Yu N Molin *Dokl. Akad. Nauk* **349** 780 (1996) [a]
39. O M Usov, Candidate Thesis in Chemical Sciences, Institute of Chemical Kinetics and Combustion, Siberian Branch of the Russian Academy of Sciences, Novosibirsk, 1997
40. O M Usov, V M Grigoryants, B M Tadjikov, Yu N Molin *Radiat. Phys. Chem.* **49** 237 (1997)
41. S V Anishchik, O M Usov, O A Anisimov, Yu N Molin *Radiat. Phys. Chem.* **51** 31 (1998)
42. V A Bagryansky, O M Usov, V I Borovkov, T V Kobzeva, Yu N Molin *Chem. Phys.* **255** 237 (2000)
43. B Brocklehurst, R S Dixon, E M Gardy, V J Lopata, M J Quinn, A Singh, F P Sargent *Chem. Phys. Lett.* **28** 361 (1974)
44. B Brocklehurst *Chem. Phys. Lett.* **28** 357 (1974)
45. V A Bagryansky, O M Usov, N N Lukzen, Yu N Molin *Appl. Magn. Reson.* **12** 505 (1997)
46. T V Kobzeva, V A Bagryansky, Yu N Molin *Dokl. Akad. Nauk* **387** 506 (2002) [a]
47. B Brocklehurst *J. Chem. Soc., Faraday Trans.* **93** 1079 (1997)
48. J M Jung *Chem. Phys. Lett.* **380** 190 (2003)
49. S V Anishchik, V M Grigoryants, I V Shebolaev, Yu D Chernousov, O A Anisimov, Yu N Molin *Pribory Tekh. Eksperim.* (4) 74 (1989)
50. V A Bagryansky, V I Borovkov, Yu N Molin, M P Egorov, O M Nefedov *Mendeleev Commun.* 132 (1997)
51. V A Bagryansky, V I Borovkov, Yu N Molin, M P Egorov, O M Nefedov *Chem. Phys. Lett.* **295** 230 (1998)
52. V A Bagryansky, V I Borovkov, Yu N Molin *Phys. Chem. Chem. Phys.* **6** 924 (2004)
53. V A Bagryansky, Doctoral Thesis in Physical and Mathematical Sciences, Kazan Physical Technical Institute, Russian Academy of Sciences, Kazan, 2006
54. V I Borovkov, V A Bagryansky, Yu N Molin, M P Egorov, O M Nefedov *Phys. Chem. Chem. Phys.* **5** 2027 (2003)
55. V I Borovkov, N P Gritsan, I V Yeletskikh, V A Bagryansky, Yu N Molin *J. Phys. Chem. A* **110** 12752 (2006)
56. V I Borovkov, N P Gritsan, V A Bagryansky, Yu N Molin *Dokl. Akad. Nauk* **413** 202 (2007) [a]
57. V I Borovkov, K L Ivanov, V A Bagryansky, Yu N Molin *J. Phys. Chem. A* **110** 4622 (2006)
58. V A Bagryansky, M M Vyushkova, I V Beregovaya, L N Shchegoleva, V I Borovkov, P A Potashov, N N Lukzen, Yu N Molin *The 5th Asia-Pacific EPR/ESR Symposium (APES 2006) (Book of Abstracts), Novosibirsk, 2006* p. 43
59. V I Borovkov, Yu N Molin *Phys. Chem. Chem. Phys.* **6** 2119 (2004)
60. V I Borovkov, Yu N Molin *Chem. Phys. Lett.* **398** 422 (2004)
61. V I Borovkov, Yu N Molin *Dokl. Akad. Nauk* **396** 633 (2004) [a]
62. V I Borovkov, I V Eletskikh *Pribory Tekh. Eksperim.* (1) 90 (2005)
63. S V Anishchik, V I Borovkov, V I Ivannikov, Yu D Chernousov, I V Shebolaev *Pribory Tekh. Eksperim.* (2007) (in the press)
64. V A Bagryansky, V I Borovkov, Yu N Molin *Dokl. Akad. Nauk* **382** 794 (2002) [a]
65. V A Bagryansky, V I Borovkov, Yu N Molin *Mol. Phys.* **100** 1071 (2002)
66. V I Borovkov, P A Potashov, L N Shchegoleva, V A Bagryansky, Y N Molin *J. Phys. Chem. A* **111** 5839 (2007)
67. B Brocklehurst *Nature (London)* **221** 921 (1969)
68. B Brocklehurst *J. Chem. Soc., Faraday Trans. 2* **72** 1869 (1976)
69. K Schulten, P G Wolynes *J. Chem. Phys.* **68** 3292 (1978)
70. D V Stass, N N Lukzen, B M Tadjikov, V M Grigoryantz, Yu N Molin *Chem. Phys. Lett.* **243** 533 (1995)
71. V A Bagryansky *Dokl. Akad. Nauk* **402** 781 (2005) [a]
72. V A Bagryansky, K L Ivanov, V I Borovkov, N N Lukzen, Yu N Molin *J. Chem. Phys.* **122** 224503 (2005)
73. M V Fedin, P A Purtov, E G Bagryanskaya *Chem. Phys. Lett.* **339** 395 (2001)
74. R A Marcus *Annu. Rev. Phys. Chem.* **15** 155 (1964)
75. Ch Slichter *Principles of Magnetic Resonance* (Heidelberg: Springer, 1978)
76. M G Townsend, S I Weissman *J. Chem. Phys.* **32** 309 (1960)
77. M R Das Stephen, B Wagner, J H Freed *J. Chem. Phys.* **52** 5404 (1970)
78. B M Tadjikov, D V Stass, Y N Molin *J. Phys. Chem. A* **101** 377 (1997)
79. Y Iwasaki, K Maeda, H Murai *J. Phys. Chem. A* **105** 2961 (2001)
80. E G Bagryanskaya, V R Gorelik, R Z Sagdeev *Chem. Phys. Lett.* **264** 655 (1997)
81. S R Shakirov, T N Makarov, E G Bagryanskaya, R Z Sagdeev *Phys. Chem. Chem. Phys.* **3** 3672 (2001)
82. T N Makarov, E G Bagryanskaya, S R Shakirov, N N Lukzen, R Z Sagdeev *Chem. Phys. Lett.* **317** 252 (2000)

[a] — *Dokl. Phys. Chem. (Engl. Transl.)*